AIP | Applied Physics Letters

Anisotropy of effective masses in CuInSe2

M. V. Yakushev, F. Luckert, A. V. Rodina, C. Faugeras, A. V. Karotki et al.

Citation: Appl. Phys. Lett. **101**, 262101 (2012); doi: 10.1063/1.4773480
View online: http://dx.doi.org/10.1063/1.4773480
View Table of Contents: http://apl.aip.org/resource/1/APPLAB/v101/i26
Published by the American Institute of Physics.

Anisotropy of effective masses in $CuInSe_2$

M. V. Yakushev,[1,a)] F. Luckert,[1] A. V. Rodina,[2] C. Faugeras,[3] A. V. Karotki,[4] A. V. Mudryi,[4] and R. W. Martin[1,b)]
[1]*Department of Physics, SUPA, Strathclyde University, G4 0NG Glasgow, United Kingdom*
[2]*A.F. Ioffe Physico-Technical Institute, 194021 St. Petersburg, Russia*
[3]*LNCMI, BP 166, 38042 Grenoble Cedex 9, France*
[4]*Scientific-Practical Material Research Centre of the National Academy of Science, P.Brovki 19, 220072 Minsk, Belarus*

(Received 20 November 2012; accepted 13 December 2012; published online 26 December 2012)

Anisotropy of the valence band is experimentally demonstrated in $CuInSe_2$, a key component of the absorber layer in one of the leading thin-film solar cell technology. By changing the orientation of applied magnetic fields with respect to the crystal lattice, we measure considerable differences in the diamagnetic shifts and effective g-factors for the A and B free excitons. The resulting free exciton reduced masses are combined with a perturbation model for non-degenerate independent excitons and theoretical dielectric constants to provide the anisotropic effective hole masses, revealing anisotropies of 5.5 (4.2) for the A (B) valence bands. © *2012 American Institute of Physics*. [http://dx.doi.org/10.1063/1.4773480]

$CuInSe_2$ is a direct band gap semiconductor used in the absorber layers of solar cells currently holding the efficiency record (20%) for thin-film photovoltaic (PV) devices.[1] Although the gap between this value and the theoretical limit of 30% (for a single-junction solar cell) is large, it also demonstrates the great potential for improvements of this technology. An important prerequisite for this advance is the understanding of fundamental electronic properties such as the energy-wave vector ($E - \boldsymbol{k}$) dispersion relations, which define the charge carrier effective masses. Their values and anisotropy have a profound influence on essential technological parameters: conductivity, charge carrier mobility, densities of states, and subsequently on the performance of electronic devices.[2]

The carrier effective masses and their anisotropy can be experimentally determined from the diamagnetic shift rates of free exciton lines in optical spectra, when magnetic fields ($\boldsymbol{B}$) are applied along different crystallographic directions, whereas splitting of the lines can clarify exciton effective g-factors, which are vital for understanding the valence band and defect properties.[3,4] Resolving free excitons corresponding to different valence sub-bands is essential for a separate analysis of each band.[4]

$CuInSe_2$ has a D_{2d} point-group chalcopyrite structure, which can be derived from the sphalerite structure of its binary analogue ZnSe by the ordered substitution of Zn by either Cu or In. The Se atoms then have two different pairs of bonds (Cu-Se and In-Se) resulting in a uniaxial tetragonal distortion of the ZnSe cubic lattice. Therefore, the chalcopyrite unit cell is doubled in one distinguished direction (z).[5] In $CuInSe_2$, the c lattice parameter along this direction is slightly longer than double that of the a lattice parameter in a perpendicular (x or y) direction. A small negative tetragonal distortion $\tau = (1 - c/2a)$ (approximately -0.5% in the studied samples) with the spin-orbit interaction, splits the triply degenerated valence band into the three sub-bands A, B, and C.

$CuInSe_2$ has been studied for more than 40 years and although some essential knowledge was gained during the early excitonic studies,[5] progress has been slowed down by a lack of high-quality single crystals. In part, this is a consequence of the complexity of the $CuInSe_2$ phase diagram. Very few reports have demonstrated resolved A and B free exciton (FX_A, FX_B) lines in the photoluminescence (PL) spectra.[6,7] Only recently has the width of the excitonic features become sufficiently narrow to usefully apply magneto-photoluminescence (MPL).[8]

The presence of a high degree of anisotropy for the hole effective mass was shown experimentally in uniaxial direct bandgap wurtzite semiconductors GaN.[9] Such anisotropy has not, as yet, been experimentally demonstrated for any chalcopyrite material although studied theoretically.[10,11] In Refs. 12 and 13, values for the hole effective masses were determined experimentally in non-oriented $CuInSe_2$. These values are different significantly from each other. In addition, since A- and B-free excitons were not resolved in the optical spectra, the quality of the $CuInSe_2$ samples used for these measurements is questionable suggesting a necessity for further studies of the hole masses and their anisotropies. Neither experimentally nor theoretically determined estimates of the g-factors for $CuInSe_2$ have so far been reported.

In this letter, we report data from high-quality $CuInSe_2$ single crystals that quantify the anisotropy of the valence band for the first time in a material with chalcopyrite symmetry. We demonstrate a considerable difference between the rates of diamagnetic shifts for FX_A in magnetic fields along ($\boldsymbol{B}//z$) and perpendicular ($\boldsymbol{B}\perp z$) to the tetragonal crystallographic direction z, and a smaller difference of the inverted character for the diamagnetic shifts of FX_B. The anisotropic FX reduced masses result in a large anisotropy of the A and B sub-band effective hole masses, calculated assuming an experimental value of the effective electron

a)Author to whom correspondence should be addressed. Electronic mail: michael.yakushev@strath.ac.uk.
b)r.w.martin@strath.ac.uk.

mass m_e combined with a theoretically predicted anisotropy. Anisotropic A and B FX effective g-factors are also estimated.

We grew bulk single crystals of $CuInSe_2$ by the vertical Bridgman technique.[14] The elemental composition of the crystals, as measured by energy dispersive X-ray analysis, was close to the ideal stoichiometry (Cu: 24.9, In: 24.9, and Se: 50.2 at. %). We established the orientation of the three main cubic structure crystallographic axes ⟨100⟩, ⟨010⟩, and ⟨001⟩ (x, y, and z, respectively) of the samples by analysis of x-ray Laue patterns. Cleaved surfaces of the crystals were examined by PL at 4.2 K. We performed MPL measurements by employing the 514 nm line of an Ar^+ laser as an excitation source and using an InGaAs array detector. In all the experiments, the propagation direction $\boldsymbol{K}$ of the laser beam was perpendicular to the tetragonal direction, z, ($\boldsymbol{K}\perp z$) and parallel to the x-axis ($\boldsymbol{K}//x$). The spectral resolution was 0.14 meV and the accuracy of the spectral line positions was about 0.2 meV. Magnetic fields up to 13 T were generated by a resistive magnet in the Laboratoire National des Champs Magnétiques Intenses. More details on the experimental set ups are provided in Refs. 8 and 28.

The evolution of the near band edge PL spectra under the influence of magnetic fields applied along the x- and z-directions of the crystalline lattice is shown in Figs. 1(a) and 1(b), respectively. These spectra reveal several sharp and well resolved lines associated with FX_A and FX_B free excitons (full width at half maximum of 1.4 meV (Ref. 7) at zero magnetic field) as well as the M1 and M2 bound excitons.[6–8] This letter focuses on FX_A and FX_B, occurring at 1.0417 eV and 1.0453 eV at zero magnetic field. As seen in Fig. 1, the application of magnetic fields results in non-linear energy shifts of the spectral positions of both the A and B excitonic lines. The PL spectra, measured for $\boldsymbol{B}$ applied along the x and y directions ($\boldsymbol{B}\perp z$), reveal the same rate of shift. However, for the $\boldsymbol{B}//z$ orientation, the rate is significantly greater, as shown in Fig. 1(c) for $\boldsymbol{B} = 13$ T, confirming that $CuInSe_2$ is a uniaxial anisotropic crystal and z-axis is the tetragonal direction of the lattice. Fig. 1 shows that FX_A splits into two lines for each of the three orientations. This splitting and shift from the 0 T position is smaller for $\boldsymbol{B}\perp z$, whereas for $\boldsymbol{B}//z$ these are considerably greater. The magnetic field dependencies of the spectral positions of the FX_A and FX_B for the $\boldsymbol{B}\perp z$ and $\boldsymbol{B}//z$ orientations are plotted in Figs. 2(a) and 2(b), respectively.

The considerable difference in the non-linear shifts of the FX_A for the $\boldsymbol{B}\perp z$ and $\boldsymbol{B}//z$ orientations is apparent, indicating a high degree of the anisotropy of the FX_A reduced mass.[3,4] The difference between the FX_B diamagnetic shifts for the two orientations is much smaller and is inverted with respect to FX_A. The inverted character of the B anisotropy can be better seen in Fig. 2(c), which shows how the difference between the spectral positions of the mid-points of the FX_A and FX_B doublets changes with the magnetic field strength. For FX_A, the difference is negative indicating that the parallel component of the diamagnetic shift is greater than the perpendicular one, whereas for FX_B the difference is small and positive indicating that the parallel component is slightly smaller than the perpendicular one.

For weak magnetic fields, the dependence of the exciton energy E_{exc} on the magnetic field strength B can be described in terms of a combination of linear Zeeman and quadratic diamagnetic shifts:

$$E_{exc}(B) = E_{exc}(0) \pm \frac{1}{2} g\mu_B B + c_d B^2, \quad (1)$$

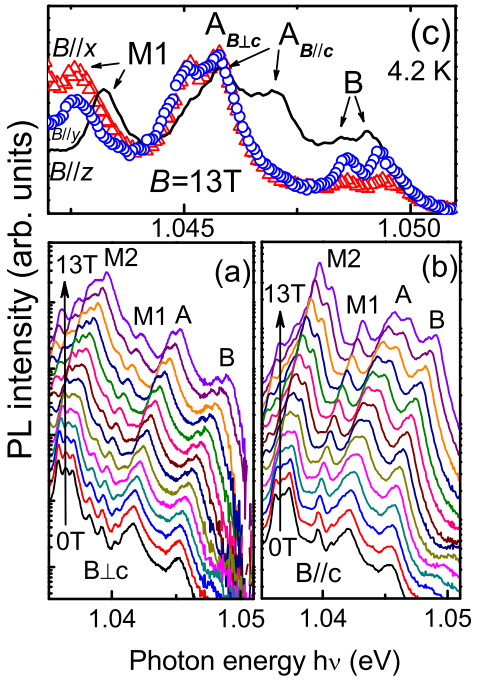

FIG. 1. Evolution of the PL spectra of the free A, B, and M1–M2 bound excitons in $CuInSe_2$ for magnetic fields $\boldsymbol{B}$ from 0 to 13 T at $\boldsymbol{B}\perp z$ (a) and $\boldsymbol{B}//z$ (b). A comparison of the PL spectra at 13 T for $\boldsymbol{B}//x$, $\boldsymbol{B}//y$, and $\boldsymbol{B}//z$ (c). The light propagation direction is $\boldsymbol{K}//x$ ($\boldsymbol{K}\perp z$).

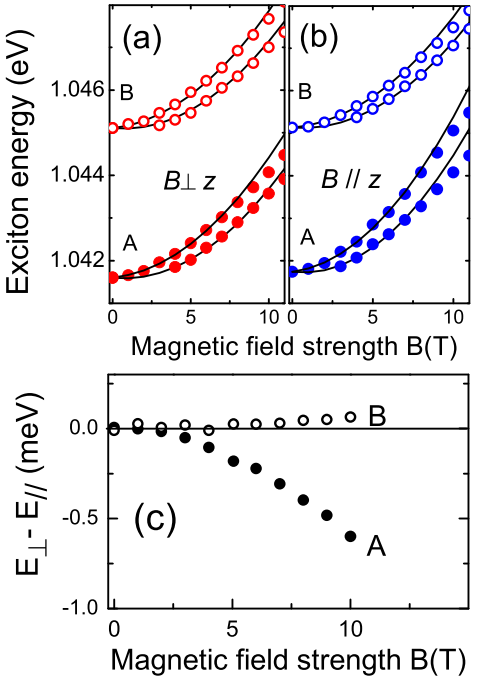

FIG. 2. Dependencies of the A and B exciton spectral positions on the magnetic field strength for $\boldsymbol{B}\perp z$ (a) and $\boldsymbol{B}//z$ (b). Symbols are experimental data, solid lines are curves calculated using Eq. (1). Difference between the FX_A and FX_B doublet mid-points for the $\boldsymbol{B}\perp z$ and $\boldsymbol{B}//z$ orientations (c).

where g is the effective Lande factor of the exciton, $\mu_B = e\hbar/(2m_0c)$ is the Bohr magneton (e is the positive electron charge, c the speed of light, and m_0 is the free electron mass), and c_d is the diamagnetic shift rate. The linear Zeeman term depends on the projection of the total exciton spin on the direction of the magnetic field and can be either positive or negative, whereas the quadratic diamagnetic shift term results from deformations of the relative motion of the electron and hole, induced by Lorentz forces is always positive[2] and proportional to the square of the exciton Bohr radius in the plane perpendicular to the direction of the field $\boldsymbol{B}$. For the ground state electron in a hydrogen atom, the diamagnetic rate is isotropic and given by, $c_d{}^0 = {}^1/_2\,\mu_B{}^2/Ry \approx 1.232 \times 10^{-10}\,\mathrm{eV\,T^{-2}}$, where $Ry = m_0 e^4/(2\hbar^2)$ is the hydrogen Rydberg energy of 13.6 eV.

The weak magnetic field limit for isotropic excitons can be determined by evaluating $\beta = \hbar\Omega/(2Ry^*)$,[15] where $\Omega = eB/(\mu c)$ and $Ry^* = Ry\mu/(m_0\varepsilon^2)$ are the exciton cyclotron frequency and effective Rydberg energy, respectively, ε is the static dielectric constant and μ the exciton reduced mass. For $\beta \ll 1$, the fields are below the weak field limit, Coulomb forces dominate and the magnetic field can be treated as a perturbation. In anisotropic materials, the values of the exciton reduced masses as well as the dielectric constants are anisotropic, while the exciton binding energy is not necessarily equal to Ry^*.[3,4,9,11] Nevertheless, we take for the estimation of $Ry^* = E_b = 8.5$ meV, the exciton binding energy from Ref. 8, and $\mu = 0.08m_0$, calculated for the electron $m_e = 0.09m_0$ (Ref. 16) and hole $m_h = 0.73m_0$ (Ref. 12) effective masses. With these parameters, we estimate the weak field limit to be valid up to approximately 7 T. We have fitted the experimental spectral positions of FX_A and FX_B at magnetic fields $\boldsymbol{B}$ varying from zero up to 7 T using Eq. (1), as shown in Figs. 2(a) and 2(b) for magnetic field oriented $\boldsymbol{B}\perp z$ and $\boldsymbol{B}//z$, respectively. At greater fields, the quadratic functions exceed the experimental energies indicating that the weak field approximation is no longer valid. Table I shows fitted values of the perpendicular and parallel components of the adjustable parameters, c_d and g, which are anisotropic for both FX_A and FX_B. The $g_\perp$ and $g_{//}$ are the components of the excitonic effective g-factor. Their analysis will be reported elsewhere.

Perturbation theories, developed for anisotropic excitons in biaxial[4] and uniaxial[3] crystals (neglecting the interaction between A and B valence subbands), predict that anisotropies of the diamagnetic shift rates are solely determined by that of the excitonic reduced masses $\mu_{//}$ and $\mu_\perp$ for the lattice directions parallel and perpendicular to z[3,4]

$$c_{d//} = \frac{\mu_B^2 m_0^2}{2Ry^*\mu_\perp^2}, \quad c_{d\perp} = \frac{\mu_B^2 m_0^2}{2Ry^*\mu_\perp\mu_{//}}. \tag{2}$$

Expressions for the averaged values of the exciton reduced mass μ and static dielectric constant ε entering the expression for Ry^* in Eq. (2) depend on the choice of the zero approximation in different perturbation models. In Ref. 4, Ry^* is calculated using

$$\frac{1}{\mu} = \frac{\varepsilon}{3}\left(\frac{2}{\mu_\perp\varepsilon_\perp} + \frac{1}{\mu_{//}\varepsilon_{//}}\right), \quad \varepsilon = (\varepsilon_{//}\varepsilon_\perp^2)^{1/3}. \tag{3}$$

Then, the $\mu_\perp$ and $\mu_{//}$ for FX_A and FX_B can be found as

$$\chi = \frac{\mu_\perp}{\mu_{//}} = \frac{c_{d\perp}}{c_{d//}}, \quad \frac{\mu_\perp}{m_0} = \left(c_d^0\varepsilon^2\frac{2+\chi\eta}{3\eta^{1/3}c_{d//}}\right)^{1/3}, \tag{4}$$

where $\eta = \varepsilon_\perp/\varepsilon_{//}$ is the anisotropy of static dielectric constants. Literature values of the dielectric constant in $CuInSe_2$ reveal significant scatter from 9.3 (Ref. 12) to 16 (Ref. 17). Therefore, the theoretical values of $\varepsilon_\perp = 11.0$ and $\varepsilon_{//} = 10.3$ (Ref. 10) have been taken to calculate $\mu_{//}$ and $\mu_\perp$ using Eqs. (2)–(4). The calculated reduced masses are shown in Table II. The reduced masses of excitons, determined from optical measurements in polar lattices, are polaron reduced values μ_p, which include carrier interaction with phonons.[2] A significant difference between $\mu_{p\perp}$ and $\mu_{p//}$ for the FX_A reduced mass manifests its anisotropic nature indicating that $\mu_{p//}$(A) is its heavier component. The anisotropy of the FX_B is smaller and inverted to that of FX_A with $\mu_{p//}$(B) being the lighter component. Exciton effective Rydbergs Ry^*(A) and Ry^*(B) are calculated to be 9.5 and 9.9 meV, respectively, and are larger than but in satisfactory agreement with the binding energies E_b of 8.5 and 8.4 meV determined from the A and B exciton excited state spectral positions.[8] The band anostropy parameters[11] $\gamma = \varepsilon_\perp\mu_\perp/(\varepsilon_{//}\mu_{//})$ are 0.82 and 1.11 for the A and B excitons, respectively. For such anisotropy, the perturbations theories are in very good agreement with more rigorous treatment of the anistropy.[11]

We now calculate values for the hole effective masses m_h using the measured FX reduced masses and literature electron effective masses. The conduction band dispersions in $CuInSe_2$, calculated by Persson[10] using a full-potential linearised augmented plane wave method, suggest a small anisotropy which is quite consistent with the experimental data $m_e = 0.09m_0$ (Ref. 16) is isotropic within the experimental errors of $\pm 0.01m_0$. Two more recent experimental measurements of m_e in non-oriented $CuInSe_2$, from the Shubnikov-de Haas effect $0.08m_0$ (Ref. 19) and the Hall coefficient temperature dependence $0.09m_0$,[20] are also in good agreement with the theoretical estimates.[10] Thus, $m_e = 0.09m_0$ (Ref. 16) with a small, anisotropy, can be considered to be reliable. As it is determined by Faraday rotation measurements, this value is a high-frequency (bare conductive band) mass m_e,[21] whereas

TABLE I. The experimental values of the diamagnetic shift rates c_d and absolute values of the exciton effective g-factors, $|g|$, for FX_A and FX_B, measured for $\boldsymbol{B}\perp z$ and $\boldsymbol{B}//z$.

Orientation	A,($B\perp z$)	A,($B//z$)	B,($B\perp z$)	B,($B//z$)
c_d ($\mathrm{eV\cdot T^{-2}}$) $\times 10^{-5}$	2.45 ± 0.02	3.19 ± 0.02	2.39 ± 0.01	2.31 ± 0.01
$\lvert g\rvert$	1.27	1.56	1.23	1.01

TABLE II. Reduced polaron μ_p masses and effective Rydbergs Ry^* of the A and B excitons.

Exciton	$\mu_{p//}/m_0$	$\mu_{p\perp}/m_0$	μ_p/m_0	Ry* (meV)
A	0.097 ± 0.003	0.074 ± 0.003	0.081 ± 0.003	9.5
B	0.083 ± 0.003	0.086 ± 0.003	0.084 ± 0.003	9.9

our MPL data require the use of the electron effective polaron masses $m_{e,hp} \approx (1+\alpha_{e,h}/6)m_{e,h}$,[2] which are slightly heavier due to carrier interaction with optical mode phonons in polar lattices. Any possible anisotropy of the Fröhlich carrier coupling constants is neglected to give $\alpha_e = 0.202$ and $\alpha_h = 0.524$, respectively, for both FX_A and FX_B assuming a longitudinal optical (LO) phonon energy of 29 meV (Ref. 22) and theoretical anisotropic components of the high-frequency dielectric constant $\varepsilon_{\infty\perp} = 8.2$ and $\varepsilon_{\infty//} = 7.8$.[10] In our calculations, we have used values of the electron effective polaron masses as $m_{e\perp p} = 0.090m_0$ and $m_{e//p} = 0.101m_0$ determined by the renormalization of the bare conduction band mass components $m_{e\perp} = 0.087m_0$ and $m_{e//} = 0.097m_0$, which were constrained to average to give $m_e = (m_{e//}m_{e\perp}^2)^{1/3} = 0.09m_0$ (the DOS value) in agreement with the experiment,[16] as well as the theoretically predicted anisotropy $m_{e\perp}/m_{e//} = 1.125$.[10] Calculations using experimental ε reported in Refs. 17 and 18 resulted in negative values of the hole masses. One of the possible reasons for it might be the neglectance of the A and B exciton coupling as the spectral splitting of FX_A and FX_B (3.6 meV) is significantly smaller than Ry^*(A) and Ry^*(B). For a more rigorous treatment such as a coupling should be taken into account, as it was done for GaN.[9] What is more, the use of the consistent expressions and experimental data for diamagnetic shift rates and exciton binding energies would allow to determine the full set of the exciton residue masses and dielectric constants simultaneously. This would be the subject of the future work.

Table III shows the perpendicular and parallel polaron mass components of the A and B holes, m_{Ap} and m_{Bp}, as well as the bare A and B valence sub-band masses m_A and m_B. Four decimal places were retained through the calculations and then the answers were rounded to three decimal places. The DOS value of the bare A-hole mass $m^*_A = 0.701m_0$ is in good agreement with $0.73m_0$ (Ref. 12) and a separate effective hole mass for the A exciton $0.71m_0$, estimated by Neumann *et al.*[23] using a theoretical approach developed for isotropic bands.[24] Our B hole masses are significantly greater than the $0.092m_0$,[23] estimated by the same approach. The hole masses calculated by Persson[10] are smaller than those determined in this study as well as those measured experimentally in Refs. 12 and 23. Our anisotropy of the A valence band ($m_{A//}/m_{A\perp} = 5.5$) is in reasonable agreement with the theoretically predicted value of 4.7.[10] The B valence band anisotropy is inverted and smaller than that for the A band as theoretically predicted,[10] although its value $m_{B\perp}/m_{B//} = 4.2$ is double the theoretical prediction of 2.1.

$CuInSe_2$ is similar to wurtzite semiconductors[9] in that the effective masses in each of the three valence subbands can be expressed using components of the effective ***kp*** Hamiltonian and splittings between these subbands.[25] Although the anisotropy is caused by the crystal field distortion, the theory predicts that the A hole mass anisotropy does not depend on the crystal field value Δ_{cf}, which in $CuInSe_2$ is very small (about 5 meV).[5] The B hole effective mass anisotropy should also be almost independent of Δ_{cf} if it is much smaller than the spin-orbit interaction Δ_{so}, which is the case for $CuInSe_2$ as reflected by the A–B and A–C exciton splitting differences.[5] The theory also predicts inversion of the B hole anisotropy with respect to that of the A hole, as observed in our experiment.

Recently reported $c_d = 2.7 \times 10^{-5}$ eV·T^{-2} for FX_A and $c_d = 2.4 \times 10^{-5}$ eV·T^{-2} for FX_B in non-oriented $CuInSe_2$ single crystals using MPL,[26] are in good agreement with the values shown in Table I. Hole masses and c_d of FX_A were also recently measured from MPL spectra for non-oriented single crystals of $CuInS_2$ (Ref. 27) and $CuGaSe_2$.[28] In $CuInS_2$ $c_d = 4.5 \times 10^{-6}$ eV·T^{-2}, calculated for FX_A using the low field approximation, is significantly smaller than that found in $CuInSe_2$ and can be explained by a smaller Bohr radius $a_B = 3.8$ nm of FX_A in $CuInS_2$.[27] In $CuInSe_2$, both the FX_A and FX_B exciton a_B are 8.5 nm.[8] In $CuGaSe_2$ the estimated $c_d = 9.82 \times 10^{-6}$ eV T^{-2} for FX_A falls between those for $CuInSe_2$ and $CuInS_2$ in accordance with its intermediate value of $a_B = 5.1$ nm.[28]

In conclusion, the diamagnetic shifts of the A and B free exciton lines in the photoluminescence spectra of $CuInSe_2$ single crystals reveal a considerable difference for magnetic fields applied perpendicular and parallel to the tetragonal direction z of the chalcopyrite lattice, providing an experimental demonstration of valence band anisotropy in $CuInSe_2$. The exciton reduced masses are calculated within the low field approximation assuming theoretical anisotropic dielectric constants and using a first order perturbation model for non-degenerate independent excitons. The A free exciton reduced mass demonstrates a strongly anisotropic nature whereas the anisotropy of the B free exciton reduced mass is weaker and inverted with respect to the orientation. Effective hole masses of $m_{A//} = 2.176m_0$ and $m_{A\perp} = 0.399m_0$ for the A, as well as $m_{B//} = 0.423m_0$, $m_{B\perp} = 1.789m_0$ for the B valence sub-bands are estimated assuming literature experimental effective electron masses combined with a small theoretical anisotropy. The determined effective g-factors are strongly anisotropic for both the A and B excitons.

TABLE III. Polaron and bare effective masses of the A- and B-band holes (m_A and m_B) as well as the DOS hole masses for these bands (m^*_A and m^*_B).

m_h/m_0	$m_{A//}$	$m_{A\perp}$	m^*_A	$m_{B//}$	$m_{B\perp}$	m^*_B
m_p	2.384	0.437	0.770	0.464	1.960	1.213
Bare	2.176	0.399	0.702	0.423	1.789	1.106

This work was supported by the EPSRC, Royal Society, Materials in Engineering (4.5.01), BCFR (F11MC-021), RFBR (10-03-96047 and 11-03-00063), and EC-EuroMagNetII-228043.

[1]P. Jackson, D. Hariskos, E. Lotter, S. Paetel, R. Wuerz, R. Menner, W. Wischmann, and M. Powalla, Prog. Photovoltaics **19**, 894 (2011).
[2]C. F. Klingshirn, *Semiconductor Optics* (Springer-Verlag, 1995).
[3]R. G. Wheeler and J. O. Dimmock, Phys. Rev. **125**, 1805 (1962).
[4]S. Taguchi, T. Gota, M. Takeda, and G. Kido, Phys. Soc. Jpn. **57**, 3256 (1988).
[5]J. L. Shay and J. H. Wernick, *Ternary Chalcopyrite Semiconductors-Growth, Electronic Properties, and Applications* (Pergamon, 1975).
[6]S. Chatraphorn, K. Yoodee, P. Songpongs, C. Chityuttakan, K. Sayavong, S. Wongmanerod, and P. O. Holtz, Jpn. J. Appl. Phys., Part 2 **37**, L269 (1998).
[7]F. Luckert, M. V. Yakushev, C. Faugeras, A. V. Karotki, A. V. Mudryi, and R. W. Martin, J. Appl. Phys. **111**, 093507 (2012).
[8]M. V. Yakushev, F. Luckert, C. Faugeras, A. V. Karotki, A. V. Mudryi, and R. W. Martin, Appl. Phys. Lett. **97**, 152110 (2010).

[9]A. V. Rodina, M. Dietrich, A. Goldner, L. Eckey, A. Hoffmann, Al. L. Efros, M. Rosen, and B. K. Meyer, Phys. Rev. B **64**, 115204 (2001).
[10]C. Persson, Appl. Phys. Lett. **93**, 072106 (2008).
[11]B. Gil, D. Felbacq, and S. F. Chichibu, Phys. Rev. B **85**, 075205 (2012).
[12]T. Irie, S. Endo, and S. Kimura, Jpn. J. Appi. Phys., Part 1 **18**, 1303 (1979).
[13]S. M. Wasim, G. Marcano, and G. S. Porras, Jpn. J. Appl. Phys., Suppl. **19**(3), 133 (1980).
[14]R. D. Tomlinson, Sol. Cells **16**, 17 (1986).
[15]R. P. Seisyan and B. P. Zakharchenya, *Landau Level Spectroscopy* (North-Holland, 1991).
[16]H. Weinert, H. Neumann, H. J. Hobler, G. Kuhn, and N. V. Nam, Phys. Status Solidi B **81**, K59 (1977).
[17]G. Riede, G. Subotta, H. Neumann, and X. N. Hoang, Solid State Commun. **28**, 449 (1978).
[18]P. W. Li, A. R. Anderson, and R. H. Plovnick, J. Phys. Chem. Solids **40**, 333 (1979).
[19]E. Arushanov, L. Essaleh, J. Galibert, J. Leotin, M. A. Arsene, J. P. Peyrade, and S. Askenazy, Appl. Phys. Lett. **61**, 958 (1992).
[20]S. M. Wasim, L. Essaleh, C. Rincoón, G. Marín, J. Galibert, and J. Leotin, J. Phys. Chem. Solids **66**, 1887 (2005).
[21]W. S. Baer, Phys. Rev. B **154**, 785 (1967).
[22]H. Tanino, T. Maeda, H. Fujikake, H. Nakanishi, S. Endo, and T. Trie, Phys. Rev. B **45**, 13323 (1992).
[23]H. Neumann, H. Subotta, W. Kissinger, V. Riede, and G. Kuhn, Phys. Status Solidi B **108**, 483 (1981).
[24]B. Lax and J. G. Mavroides, Phys. Rev. **100**, 1650 (1955).
[25]G. L. Bir and G. E. Pikus, *Symmetry and Strain Induced Effects in Semiconductors* (Wiley, 1974).
[26]M. V. Yakushev, R. W. Martin, A. Babinski, and A. V. Mudryi, Phys. Status Solidi C **6**, 1086 (2009).
[27]M. V. Yakushev, R. W. Martin, and A. V. Mudryi, Appl. Phys. Lett. **94**, 042109 (2009).
[28]F. Luckert, M. V. Yakushev, C. Faugeras, A. V. Karotki, A. V. Mudryi, and R. W. Martin, Appl. Phys. Lett. **97**, 162101 (2010).